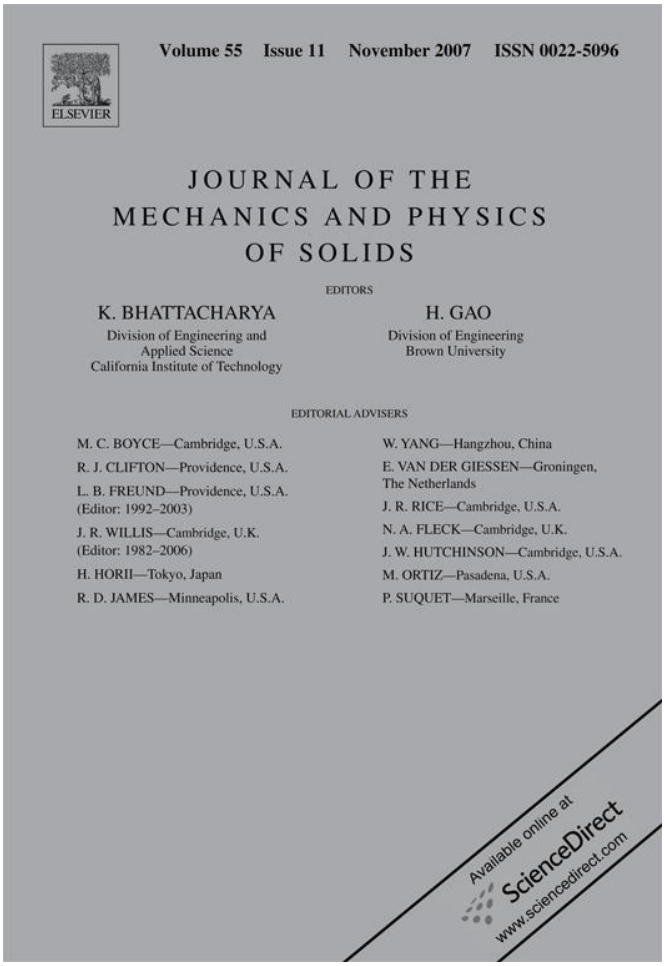

Available online at www.sciencedirect.com
ScienceDirect
Journal of the Mechanics and Physics of Solids
55 (2007) 2328–2350

JOURNAL OF THE MECHANICS AND PHYSICS OF SOLIDS

www.elsevier.com/locate/jmps

On the possibility of piezoelectric nanocomposites without using piezoelectric materials

N.D. Sharma, R. Maranganti, P. Sharma*

Department of Mechanical Engineering, University of Houston, Houston, TX 77204, USA

Received 11 December 2006; received in revised form 25 March 2007; accepted 28 March 2007

Abstract

In this work, predicated on nanoscale size-effects, we explore the tantalizing possibility of creating apparently piezoelectric composites without using piezoelectric constituent materials. In a piezoelectric material an applied *uniform* strain can induce an electric polarization (or vice-versa). Crystallographic considerations restrict this technologically important property to non-centrosymmetric systems. *Non-uniform strain* can break the inversion symmetry and induce polarization even in non-piezoelectric dielectrics. The key concept is that *all* dielectrics (including non-piezoelectric ones) exhibit the aforementioned coupling between strain gradient and polarization—an experimentally verified phenomenon known in some circles as the flexoelectric effect. This flexoelectric coupling, however, is generally very small and evades experimental detection unless very large strain gradients (or conversely polarization gradients) are present. Based on a field theoretic framework and the associated Greens function solutions developed in prior work, we quantitatively demonstrate the possibility of "designing piezoelectricity," i.e. we exploit the large strain gradients present in the interior of composites containing nanoscale inhomogeneities to achieve an overall non-zero polarization even under an uniformly applied stress. We prove that the aforementioned effect may be realized only if both the shapes and distributions of the inhomogeneities are non-centrosymmetric. Our un-optimized quantitative results, based on limited material data and restrictive assumptions on inhomogeneity shape and distribution, indicate that apparent piezoelectric behavior close to 10% of Quartz may be achievable for inhomogeneity sizes in the 4 nm range. In future works, it is not

*Corresponding author. Tel.: +1 713 743 4256.
E-mail address: psharma@uh.edu (P. Sharma).

doi:10.1016/j.jmps.2007.03.016

unreasonable to expect enhanced performance based on optimization of shape, topology and appropriate material selection.

Keywords: Piezoelectric composite; Flexoelectricity; Homogenization

1. Introduction and central concept

Non-centrosymmetry is a necessary condition for a crystal to exhibit piezoelectricity, where an applied *uniform* strain induces electric polarization (or vice versa). Here the polarization vector **P** is related to the second-order strain tensor **ε** through the third-order piezoelectric tensor **p** (Nye, 1985)

$$P_i = p_{ijk}\varepsilon_{jk}. \tag{1}$$

Tensor transformation properties require that under inversion-center symmetry, all odd-order tensors vanish. Thus, most common materials, e.g. Silicon, and NaCl are not piezoelectric whereas ZnO and GaAs are. The simple schematic in Fig. 1 illustrates the molecular origins of the classical piezoelectric effect. However, it is possible to visualize how a *non-uniform strain* or the presence of *strain gradients* may potentially break the inversion symmetry and induce polarization even in *centrosymmetric* crystals (Fig. 2). Formally, this is tantamount to extending Eq. (1) to include strain gradients

$$P_i = \underbrace{p_{ijk}\varepsilon_{jk}}_{=0,\ \text{for non-piezo materials}} + \mu_{ijkl}\frac{\partial \varepsilon_{jk}}{\partial x_l}. \tag{2}$$

Here μ_{ijkl} are the so-called flexoelectric coefficients. Although the components of the third-ordered tensor '**p**' (piezoelectric coefficients) are non-zero for only selected (piezoelectric) dielectrics, the flexoelectric coefficients (components of the fourth-order tensor '**μ**') are non-zero for all dielectrics. This implies that under a non-uniform strain, at

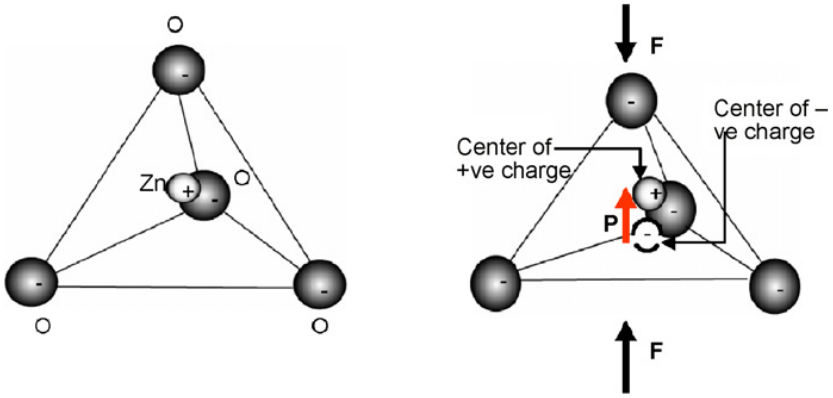

Fig. 1. Illustration of "Classical" piezoelectricity. The left figure shows the tetrahedrally coordinated cation–anion unit of a ZnO crystal. The center of negative charge of the oxygen (O) anions coincides with the center of positive charge, which is located at the Zinc (Zn) ion. Thus, there is no net dipole polarization in the absence of external pressure. Upon application of external pressure, the centers of positive and negative charge suffer relative displacement with respect to each other thereby inducing a dipole moment. Such dipole moments are induced throughout the crystal lattice thereby giving rise to net polarization.

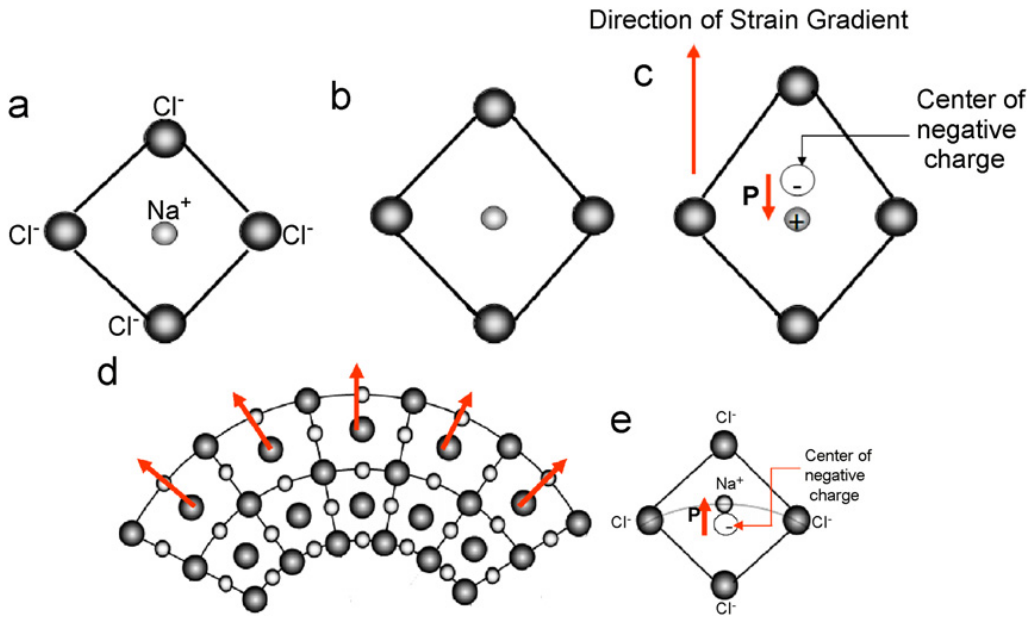

Fig. 2. (a) Undeformed NaCl unit cell. The sodium ion is positively charged while the four neighboring chlorine ions are negatively charged. As can be seen, the center of gravities of the negative charge and the positive charge coincide leading to (expectedly) zero net dipole moment. (b) Uniform Strain: application of a uniform strain displaces the identical ions equally from the center of inversion and hence the centers of the negative and positive charges coincide again thereby resulting in zero net polarization implying that NaCl is non-piezoelectric. (c) NaCl unit cell under non-uniform stretching. Application of a non-uniform strain however results in relative displacement of the centers of the negative charge and positive charge with respect to each other. This results in a dipole moment (represented by the thick red arrow) in the direction opposite to the strain gradient for the considered cell. (d) and (e) Polarization due to bending.

least in principle, all dielectric materials are capable of producing a polarization. The reader is referred to our recent work (Maranganti et al., 2006) that discusses flexoelectricity in detail although essential concepts are summarized here as well.

The universal strain gradient—polarization coupling can be interpreted from the point of view of two length scales: (i) at the length scale of a single (or few) unit cell(s), (ii) at a coarser length spanning many individual crystalline unit cells, i.e. the dimension of a nanostructure or larger. At the unit cell level, Fig. 2 illustrates how NaCl (which is non-piezoelectric) will yield zero net dipole moment (and hence no polarization) under application of uniform strain but will exhibit an apparent piezoelectric effect when subjected to strain gradients, e.g. bending or inhomogeneous stretching. At a coarser length scale, the effect of individual unit cells is accounted for in the phenomenologically introduced flexoelectric coefficients (Eq. (2)). As long as the flexoelectric coefficients are non-negligible, a finite polarization will manifest at coarser scales provided the nanostructures *are properly designed*. By proper design, we imply that the overall symmetry of the nanostructure must be such that the average of the polarization due to the presence of strain gradients is non-zero. For example, a heterogeneous spherical particle consisting of two different non-piezoelectric materials when subjected to uniform stress will exhibit spatially varying polarization due to flexoelectricity. The polarization will be significant if the particle is in the nanoscale size and if the difference in the dielectric and elastic properties of the constituents is large since the strain gradients will then be large. However, symmetry indicates that the net average polarization will regardless be zero.

Thus, "proper design" in the present context refers to (i) optimum topology, (ii) optimum differences in the material properties of the constituents that comprise the nanostructures, and (iii) optimum size.

Fig. 3 illustrates the main principle from a coarse-grained perspective.

Consider a composite consisting of two or more different non-piezoelectric dielectric materials. Even under application of uniform stress, a non-uniform strain distribution will be generated in this system. Due to the presence of strain gradients and the flexoelectric coupling, polarization will ensue. For "properly designed" nanocomposites, the net average polarization will be non-zero. Thus, the nanostructure will exhibit an overall electromechanical coupling under uniform stress behaving like an "apparently" piezoelectric material. The individual constituents must be at the nanoscale since this concept requires very large strain gradients and those (for a given strain) are generated easily only for small-scale structures.

Both mathematically (Eq. (2)) and physically (Figs. 2 and 3), it is *manifestly possible* to induce electric fields in non-piezoelectrics via strain gradients. The next logical question is how significant is this effect? As will be quantitatively demonstrated in later section, this effect is of appreciable amount (for most dielectric materials) only at the nanoscale and thus is most relevant in the context of nanostructures. Due to the role of gradients, flexoelectricity is essentially a size-effect and negligible at supra-nano length scales (for most ordinary dielectrics). Consider a structure with certain mechanical boundary conditions; the mechanical strain can be considered to be roughly the same if the system is shrunk self-similarly from mm's to nm's. However, the strain *gradient* will increase by six orders of magnitude! Incidentally, the statement regarding size-independence of strain is not *strictly* true (e.g. Zhang and Sharma, 2005a, b, Sharma et al., 2003); there is a size-dependency to strain at the nanoscale but that does not influence the point we are trying to make here, i.e. even if strain were size-independent, the strain gradient scales inversely with size. Flexoelectric coefficients are not readily available but some reasonable estimates are known for graphene (Dumitrica et al., 2002) and NaCl (Askar and Lee, 1970). Choosing the latter as an example, we can calculate its electromechanical coupling coefficient under applied voltage. One would expect it to be zero since NaCl is non-piezoelectric. However, if the flexoelectric effect is properly taken into account, it can be inferred that at 10 nm thickness, the electromechanical coupling factor reaches 80% of the value of Quartz or alternatively 12% of lead zirconate titanate (PZT) (Mindlin, 1968).

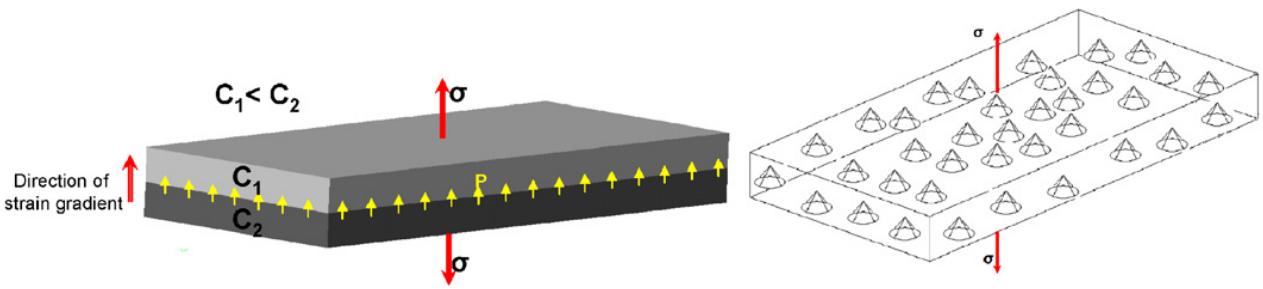

Fig. 3. Through suitable topology, arrangement, constituent property difference and selection of optimum size, heterogeneous nanostructures (i.e. bi-laminate or film with conical inclusions) such as shown in the figure can be created that will yield an "apparently" piezoelectric behavior despite the constituents being non-piezoelectric. Here C_1 and C_2 denote the 'elastic constants' of the two materials considered. The second figure is adapted from paper by Cross and co-workers (Fousek, et al., 1999, Cross, 2006).

The flexoelectric phenomenon has been experimentally observed during bending of crystal plates (e.g. Bursian and Trunov, 1974) and measurements on thin films (Catalan et al., 2004). Mindlin (1968) used the converse of the flexoelectric effect to explain the anomalous capacitance measurements of thin dielectric films while Yakobson and coworkers employed it to discuss the polarization in curved carbon shells (Dumitrica et al., 2002). Experiments with dislocated non-piezoelectric dielectric crystals have attributed overall electromechanical coupling to polarization in the vicinities of dislocations (e.g. Whitworth, 1964; Nowick and Heller, 1965; Bauer and Brantley, 1970; Robinson et al., 1978).[1] The flexoelectric effect may also be used to provide an explanation for the size-dependent piezoelectric behavior of boron nitride nanotubes (Nakhmanson et al., 2003). The aforementioned works are related to crystalline materials. As an aside, we note here that a large literature also exists in the liquid crystal and biological membrane context. It is noteworthy though that the term, "flexoelectricity" for crystalline materials was coined inspired by similar phenomenon in liquid crystals (Meyer, 1969; Schmidt et al., 1972; Indenbom et al., 1981).

Kogan (1963) has argued that for all dielectrics, e/a ($\approx 10^{-9}$ C/m) is an appropriate lower bound for the flexoelectric coefficients, where e is the electronic charge and a is the lattice parameter. Later experiments (Ma and Cross, 2001a) and simple linear chain models of ions (Marvan and Havranek, 1997) suggested multiplication by relative permittivity for normal dielectrics. Much larger magnitudes ($\approx 10^{-6}$ C/m) of flexoelectric coefficients than this lower bound are observed in certain ceramics (Ma and Cross, 2001b, 2002, 2003). Electric field created in non-piezoelectric $CaWO_4$ crystals with 4/m symmetry by applying a twisting moment was experimentally measured by Zheludev et al. (1969), which though closely related to flexoelectricity, was attributed mainly to disappearance of centrosymmetry due to applied torsion. Marvan and Havranek (1988) found presence of flexoelectric effect in an isotropic elastomer with flexoelectric coefficients roughly of the order of e/a. Flexoelectricity, of course also exists in materials that are already piezoelectric and in fact experimental evidence suggests that flexoelectric coefficients are unusually high in such materials—see the experimental work of Cross and co-workers (2001a, b, 2002, 2003, 2006) on ferroelectric perovskites like PMN, PZT, and BST. In fact, the notion of creating "apparently piezoelectric" composites without using piezoelectric constituents appears to have first appeared in a work by Fousek et al. (1999) and more recently in work by Zhu et al. (2006) who have experimentally realized this concept.[2]

Lattice level "shell" type models of crystalline dielectrics clearly indicate that the long wavelength limit of the lattice dynamical results do not lead to the classical piezoelectric theory, which from an atomistic point of view, is simply the long wavelength representation of the core–core interactions while core–shell and shell–shell interactions are neglected (Cochran and Cowley, 1962; Dick and Overhauser, 1958; Tolpygo, 1962). To tackle this discrepancy, Mindlin (1968) introduced a continuum field theory that incorporates coupling of polarization gradients to strain (or in our language—the converse flexoelectric effect). This theory is found to correctly represent the core–shell and shell–shell interactions within a continuum field-theoretic formalism (see also the

[1]For this to occur, a necessary requirement is that the crystalline solid contain an excess of dislocation of a certain sign.

[2]This was brought to our attention by one of the anonymous referee's at an advanced stage of the peer-review process.

study of Askar and Lee, 1970). It should be noted that Mindlin's theory does not incorporate the direct flexoelectric effect or the strain gradient-polarization coupling discussed earlier. Several work subsequently expanded on Mindlin's original theory. Askar et al. (1971) considered elastic and dielectric state of cylindrical and spherical cavities as well as cracks. In a later paper, using lattice dynamical methods, the same authors also evaluated the material constants of Mindlin's theory for KCl and NaCl (1974). From the view-point of condensed matter physics, Tagantsev (1986, 1991) has proposed a phenomenological description and, in addition to providing a review, clarified several concepts related to both flexoelectricity and piezoelectricity based upon microscopic considerations.

Yet another electromechanical coupling effect which deserves mention is the well-known phenomena of electrostriction (Maugin, 1988) which is also universal for dielectrics. Electrostriction is a nonlinear effect and becomes operative at very high electric fields—the developed strain depends on the square of the electric field and consequently the direction of the electric field is independent of the sign of the strain (compression versus tension). In addition, an inverse electrostriction effect does not exist, i.e. deformation does not produce an electric field. This nonlinear effect is ignored in the present work since we only consider linearized theories and thus small strains (although not small *strain gradients*).

In the present work, based on a field theoretic framework and the associated Greens function solutions developed in prior work (Maranganti et al., 2006), we quantitatively demonstrate the possibility of "designing piezoelectricity," i.e. we exploit the large strain gradients present in the interior of composites containing nanoscale inhomogeneities to achieve an overall non-zero polarization even under applied uniform stress. We show that the governing equations for flexoelectricity demand that the inhomogeneity shape must be non-centrosymmetric for a non-zero average polarization.

The paper is organized as follows. In Section 2, we discuss the mathematical framework and the governing equations for the extended theory of electromechanical coupling. In Section 3, we develop solutions for the embedded inclusion problem subject to dilatational transformation strain. Centrosymmetric (spherical) and non-centrosymmetric (orthogonal polyhedral) shapes are used to demonstrate that to obtain non-zero average polarization in the aforementioned "meta material", the requirement of material non-centrosymmetry is transferred to requirement of shape non-symmetry of the inhomogeneity and topology arrangement. In Section 4, we propose a simple proof of this proposition. The homogenization scheme used to obtain quantitative results is discussed in Section 5 while the numerical calculations are presented in Section 6. We conclude in Section 7.

2. Mathematical framework and governing equations

Assuming an isotropic centrosymmetric[3] dielectric, the most general expression for the linearized internal energy density function Σ incorporating terms involving first gradients of the deformation gradient and the polarization is (Sahin and Dost, 1988)

$$\Sigma = \tfrac{1}{2}a_{kl}P_kP_l + \tfrac{1}{2}b_{ijkl}P_{i,j}P_{k,l} + \tfrac{1}{2}c_{ijkl}\varepsilon_{ij}\varepsilon_{kl} + d_{ijkl}P_{i,j}\varepsilon_{kl} + f_{ijkl}P_iu_{j,kl} + \tfrac{1}{2}g_{ijklmn}u_{i,jk}u_{l,mn} \tag{3}$$

[3]Thus, the material is non-piezoelectric.

$\boldsymbol{u}$ and $\boldsymbol{P}$ being displacement and polarization vectors respectively, ε_{ij} are the components of the infinitesimal strain tensor $\boldsymbol{\varepsilon}$ defined as

$$\varepsilon_{ij} = \tfrac{1}{2}(u_{i,j} + u_{j,i}). \tag{4}$$

Unless stated otherwise, Cartesian basis is used throughout and both index and direct notation will be used as convenient. '$\boldsymbol{a}$' is second-order reciprocal dielectric susceptibility, '$\boldsymbol{c}$' is fourth-order elastic constant tensor, '$\boldsymbol{d}$' is the tensor corresponding to higher-order electro-elastic couplings which link gradients of polarization to strains, '$\boldsymbol{b}$' is the tensor corresponding to the converse flexoelectric effect and is thus coupled to polarization gradients, '$\mathbf{f}$' is the tensor of flexoelectric coefficients, while '$\mathbf{g}$' dictates purely elastic nonlocal effects corresponding to the strain gradient elasticity theories. The extended theory implicit in Eq. (3) differs from classical theory of piezoelectricity in that characteristic length scales appear and (as expected and desired) results are size-dependent. Such formalism is a modified version of Mindlin's framework (Mindlin, 1968) and has been further developed in our earlier work (Maranganti et al., 2006).

Neglecting the purely elastic nonlocal effects (i.e. '$\mathbf{g}$') for an isotropic continuum occupying domain Ω and boundary S, standard variational analysis of Eq. (3) can be used to obtain the following system of equilibrium equations, boundary conditions and constitutive relations:

Equilibrium equations:

$$\begin{aligned}
&\left(t_{ij} - t_{jim,m}\right)_{,j} + F_i = 0,\\
&E_{ij,j} + E_i - \phi_{,i} + E_i^0 = 0,\\
&-\varepsilon_0\phi_{,ii} + P_{i,i} = 0 \quad \text{in } \Omega,\\
&\phi_{,ii} = 0 \quad \text{in } \Omega^*,
\end{aligned} \tag{5a–d}$$

where ϕ, $\mathbf{E}^0$, $\mathbf{F}$ are the electric potential, external electric field and external force respectively, t_{ij}, E_i and P_i are the components of the stress tensor, effective local electric field and the polarization vector respectively while E_{ij} and t_{ijm} represents the higher-order local electric force and stress, which includes higher-order gradients of the displacement vector (like $u_{i,jm}$), respectively. Note that these electromechanical stresses are defined as the partials of Σ with respect to the of respective field vectors as

$$\begin{aligned}
&t_{ij} \equiv \frac{\partial \Sigma}{\partial e_{ij}}, \quad t_{ijm} \equiv \frac{\partial \Sigma}{\partial u_{i,jm}},\\
&E_{ij} \equiv \frac{\partial \Sigma}{\partial P_{i,j}}, \quad E_i \equiv \frac{\partial \Sigma}{\partial P_i}.
\end{aligned} \tag{6a–d}$$

Boundary conditions:

$$\begin{aligned}
&n_i\sigma_{ij} = t_j,\\
&n_i E_{ij} = 0,\\
&n_i\left(\llbracket \varepsilon_0\phi_{,i} \rrbracket + P_i\right) = 0
\end{aligned} \tag{7a–c}$$

$\mathbf{n}$ and $\mathbf{t}$ are the exterior normal unit vector and the surface traction vector, respectively; ε_0 is the dielectric constant and the symbol $\llbracket\ \rrbracket$ denotes the jump across the surface S.

Constitutive relations:

$$\begin{aligned}
t_{ij} &= \left[c_{12}\delta_{ij}\delta_{ps} + 2c_{44}\delta_{ip}\delta_{js}\right]u_{p,s} + \left[d_{12}\delta_{ij}\delta_{ps} + d_{44}\left(\delta_{is}\delta_{jp} + \delta_{js}\delta_{ip}\right)\right]P_{p,s},\\
t_{ijm,m} &= \left[f_{12}\delta_{pi}\delta_{js} + f_{44}\left(\delta_{ps}\delta_{ji} + \delta_{is}\delta_{jp}\right)\right]P_{p,s},\\
E_{ij} &= \left[d_{12}\delta_{ij}\delta_{ps} + d_{44}\left(\delta_{is}\delta_{jp} + \delta_{js}\delta_{ip}\right)\right]u_{p,s}\\
&\quad + \left[b_{12}\delta_{ij}\delta_{ps} + (b_{44} + b_{77})\delta_{is}\delta_{jp} + (b_{44} - b_{77})\delta_{js}\delta_{ip}\right]P_{p,s},\\
E_i &= -\left(aP_i + \left[f_{12}\delta_{ij}\delta_{ps} + f_{44}\left(\delta_{is}\delta_{jp} + \delta_{js}\delta_{ip}\right)\right]u_{j,ps}\right).
\end{aligned} \tag{8a–d}$$

Eqs. (8a–d) can be combined with Eqs. (5a–d) to yield the following Navier-like governing equations:

$$\begin{aligned}
&c_{44}\nabla^2\mathbf{u} + (c_{12} + c_{44})\nabla\nabla\mathbf{u} + (d_{44} - f_{12})\nabla^2\mathbf{P} + (d_{12} + d_{44} - 2f_{44})\nabla\nabla\mathbf{P} + \mathbf{F} = 0,\\
&(d_{44} - f_{12})\nabla^2\mathbf{u} + (d_{12} + d_{44} - 2f_{44})\nabla\nabla\mathbf{u} + (b_{44} + b_{77})\nabla^2\mathbf{P}\\
&\quad + (b_{12} + b_{44} - b_{77})\nabla\nabla\mathbf{P} - a\mathbf{P} - \nabla\phi + \mathbf{E}^0 = 0,\\
&\quad - \varepsilon_0\nabla^2\phi + \nabla\mathbf{P} = 0.
\end{aligned} \tag{9a–c}$$

It should be noted that the displacement and polarization fields are coupled through the constants **d** and **f**. Eq. (9a–c) can be rewritten as

$$\begin{aligned}
&C_{ij}u_j + D_{ij}P_j + F_i = 0,\\
&D_{ij}u_j + B_{ij}P_j - \phi_{,i} + E_i^0 = 0,\\
&-\varepsilon_0\phi_{,ii} + P_{i,i} = 0,
\end{aligned} \tag{10a–c}$$

where

$$\begin{aligned}
C_{ji} &= C_{jpis}\nabla_p\nabla_s = \left[c_{12}\delta_{jp}\delta_{is} + c_{44}\left(\delta_{ps}\delta_{ij} + \delta_{js}\delta_{ip}\right)\right]\nabla_p\nabla_s,\\
D_{ji} &= D_{jpis}\nabla_p\nabla_s = \left[\left(d_{12} + d_{44} - 2f_{44}\right)\delta_{jp}\delta_{is} + (d_{44} - f_{12})\delta_{ps}\delta_{ij}\right]\nabla_p\nabla_s,\\
B_{ji} &= B_{jpis}\nabla_p\nabla_s - a\delta_{ij} = \left[b_{12}\delta_{jp}\delta_{is} + (b_{44} + b_{77})\delta_{ps}\delta_{ij} + (b_{44} - b_{77})\delta_{js}\delta_{ip}\right]\nabla_p\nabla_s - a\delta_{ij}.
\end{aligned} \tag{11a–c}$$

These equations may be solved, in analogy with Kelvin's solution in the theory of linearized elasticity by appropriate Green's functions. We can define two sets of Green's functions $\{G_{in}^1, G_{in}^2, \phi_n^f\}$ and $\{G_{in}^3, G_{in}^4, \phi_n^E\}$ corresponding to Eqs. (10a–c) as follows:

$$\begin{aligned}
&C_{ji}G_{in}^1(\mathbf{x} - \mathbf{x}') + D_{ji}G_{in}^2(\mathbf{x} - \mathbf{x}') + \delta_{jn}\delta(\mathbf{x} - \mathbf{x}') = 0,\\
&D_{ji}G_{in}^1(\mathbf{x} - \mathbf{x}') + B_{ji}G_{in}^2(\mathbf{x} - \mathbf{x}') - \nabla_j\phi_n^f(\mathbf{x} - \mathbf{x}') = 0,\\
&-\varepsilon_0\nabla^2\phi_n^f(\mathbf{x} - \mathbf{x}') + \nabla_i G_{in}^2(\mathbf{x} - \mathbf{x}') = 0,\\
&C_{ji}G_{in}^3(\mathbf{x} - \mathbf{x}') + D_{ji}G_{in}^4(\mathbf{x} - \mathbf{x}') = 0,\\
&D_{ji}G_{in}^3(\mathbf{x} - \mathbf{x}') + B_{ji}G_{in}^4(\mathbf{x} - \mathbf{x}') - \nabla_j\phi_n^E(\mathbf{x} - \mathbf{x}') + \delta_{jn}\delta(\mathbf{x} - \mathbf{x}') = 0,\\
&-\varepsilon_0\nabla^2\phi_n^E(\mathbf{x} - \mathbf{x}') + \nabla_i G_{in}^4(\mathbf{x} - \mathbf{x}') = 0.
\end{aligned} \tag{12a–f}$$

As evident, the first three equations (12a–c) are the Navier-like equations for the displacement, polarization and the potential fields corresponding to a *unit point force* (denoted by a delta function). Similarly, Eqs. (12d–f) are the governing equations for the displacement, polarization and the potential fields corresponding to a *unit point electrical field*.

In our previous work (Maranganti et al., 2006) we have derived analytical expressions for the Green's functions corresponding to the Lagrangian of Eq. (3) which includes pure strain-gradient terms (coupled by the tensor **g**). Neglecting these purely nonlocal terms the Green's functions become

$$
\begin{aligned}
4\pi G^{(1)}_{ij} &= \partial_i\partial_j\left[C^{(01)}R + C^{(11)}I_1 - C^{(12)}I_2\right] + \delta_{ij}\nabla^2\left[C^{(02)}R + C^{(12)}I_2\right],\\
4\pi G^{(2)}_{ij} &= 4\pi G^{(3)}_{ij} = \partial_i\partial_j\left[C^{(21)}I_1 + C^{(22)}I_2\right] - \delta_{ij}\nabla^2\left[C^{(22)}I_2\right],\\
4\pi G^{(4)}_{ij} &= \partial_i\partial_j\left[\frac{I_1}{a+(\varepsilon_0)^{-1}} - \frac{I_2}{a}\right] + \delta_{ij}\nabla^2\left[\frac{I_2}{a}\right]
\end{aligned}
\tag{13a–c}
$$

which are same as those derived by Nowacki and Hsieh (1986). The coefficients $C^{(ij)}$ and expression I_a have been defined in Appendix A.

3. Illustrative solutions for centrosymmetric (spherical) and noncentrosymmetric (orthogonal polyhedral) inclusion

Consider an arbitrary shaped *inclusion* with a prescribed stress-free transformation strain $\boldsymbol{\varepsilon}^*$ in its domain (Ω), located in an infinite isotropic medium. Here we follow the convention that the word "inclusion" refers to an embedded region that has the same mechanical and dielectric properties as the surrounding material but with a transformation strain or polarization prescribed within its domain while the word "inhomogeneity" is referred to as an embedded region with material properties differing from the surrounding matrix. Following Eshelby's (1957) well-known formalism, given a uniform transformation strain, the displacement $u_i(\mathbf{x})$ and the polarization field $P_i(\mathbf{x})$ can be written as

$$
\begin{aligned}
u_i(\mathbf{x}) = &-\int\left[c_{12}\delta_{jl}\delta_{mn} + 2c_{44}\delta_{jm}\delta_{ln}\right]\varepsilon^*_{mn}(\mathbf{x}')G^1_{ij,l}(\mathbf{x}-\mathbf{x}')\,\mathrm{d}\mathbf{x}'\\
&-\int\left[\left(d_{12}-f_{44}\right)\delta_{jl}\delta_{mn} + \left(2d_{44}-f_{12}-f_{44}\right)\delta_{jm}\delta_{ln}\right]\varepsilon^*_{mn}(\mathbf{x}')G^2_{ij,l}(\mathbf{x}-\mathbf{x}')\,\mathrm{d}\mathbf{x}'
\end{aligned}
\tag{14}
$$

and

$$
\begin{aligned}
P_i(\mathbf{x}) = &-\int\left[c_{12}\delta_{jl}\delta_{mn} + 2c_{44}\delta_{jm}\delta_{ln}\right]\varepsilon^*_{mn}(\mathbf{x}')G^3_{ij,l}(\mathbf{x}-\mathbf{x}')\,\mathrm{d}\mathbf{x}'\\
&-\int\left[\left(d_{12}-f_{44}\right)\delta_{jl}\delta_{mn} + \left(2d_{44}-f_{12}-f_{44}\right)\delta_{jm}\delta_{ln}\right]\varepsilon^*_{mn}(\mathbf{x}')G^4_{ij,l}(\mathbf{x}-\mathbf{x}')\mathrm{d}\mathbf{x}',
\end{aligned}
\tag{15}
$$

where $\{G^1_{in}, G^2_{in}, G^3_{in}, G^4_{in}\}$are defined as the set of Green's functions corresponding to Eqs. (12a–f) and are defined in Eqs. (13a–c).

Now, for a given transformation strain the polarization P_i for an inclusion of any shape can be written in terms of potentials $\phi(x)$, $\psi(x)$, $M^a(x)$ as

$$
\begin{aligned}
P_i(\mathbf{x}) = &-(3c_{12}+2c_{44})\varepsilon^*\partial_i\left(A^{(2)}\phi_{,kk} + C^{(2)}M^1_{,kk} + D^{(2)}M^2_{,kk}\right)\\
&-\left[3\left(d_{12}-f_{12}\right)+2\left(d_{44}-f_{44}\right)\right]\varepsilon^*\partial_i\left(A^{(3)}\phi_{,kk} + C^{(3)}M^1_{,kk} + D^{(3)}M^2_{,kk}\right),
\end{aligned}
\tag{16}
$$

where

$$\phi(x)=\frac{1}{4\pi}\int_{\Omega}\frac{1}{R}\,\mathrm{d}x',\quad \psi(x)=\frac{1}{4\pi}\int_{\Omega}R\,\mathrm{d}x',\quad M^{a}(x)=\frac{1}{4\pi}\int_{\Omega}\frac{\mathrm{e}^{-R/l_a}}{R}\,\mathrm{d}x' \tag{17a–c}$$

R is $|\mathbf{x}-\mathbf{x}'|$ and l_a are the length scale parameters defined in Appendix A.

It is important to note that the inclusion geometry dependence of Eq. (16) is buried within the definitions of the potentials $\phi(x)$, $\psi(x)$ and $M^{a}(x)$. Thus the solution of the polarization field of an embedded transformed inclusion is reduced entirely to the determination of the three potentials. The first two are merely the Newtonian (i.e. Harmonic) and Biharmonic potential for the inclusion shape while the third is the lesser known and harder to evaluate Yukawa potential. Closed form expressions for the Newtonian and Biharmonic potential exist for a variety of shapes (see for example, Mura, 1987) while only spherical and circular shape is amenable to analytical reduction in the case of Yukawa potential (e.g. Gibbons and Whiting, 1981; Cheng and He, 1997).

Andreev and Downes (1999), in connection with quantum dot structures, suggested a general analytical method using Fourier transform technique that allows straightforward separation of shape effects. The characteristic function for the inclusion $\chi(\mathbf{r})$ is defined as

$$\chi(\mathbf{r})=\begin{cases}1, & \mathbf{r}\in\Omega,\\ 0, & \mathbf{r}\notin\Omega.\end{cases} \tag{18}$$

The Fourier transform of the characteristic function is

$$\hat{\chi}(\mathbf{q})=\int_{\Omega}\mathrm{e}^{-\mathrm{i}\mathbf{q}\mathbf{x}}\,\mathrm{d}V(\mathbf{x}). \tag{19}$$

The polarization field (Eq. (16)) can be re-written in Fourier space as

$$\widehat{P_i(\mathbf{q})}=\mathrm{i}q_iq_kq_k\hat{\chi}(\mathbf{q})\varepsilon^{*}\left\{\begin{array}{l}\tilde{c}\left(A^{(2)}\widehat{\phi(\mathbf{q})}+C^{(2)}\widehat{M^{1}(\mathbf{q})}+D^{(2)}\widehat{M^{2}(\mathbf{q})}\right)\\ \quad+\tilde{d}\left(A^{(3)}\widehat{\phi(\mathbf{q})}+C^{(3)}\widehat{M^{1}(\mathbf{q})}+D^{(3)}\widehat{M^{2}(\mathbf{q})}\right)\end{array}\right\}, \tag{20}$$

where

$$\tilde{c}=(3c_{12}+2c_{44}),\quad \tilde{d}=\left(3\left(d_{12}-f_{12}\right)+2\left(d_{44}-f_{44}\right)\right).$$

Thus, substituting Eqs. (17a–c) in Eq. (16) and transforming to Fourier space (Kleinert, 1989), we obtain the following analytical expression for the polarization:

$$\widehat{P_i(\mathbf{q})}=\mathrm{i}q_iq_kq_k\hat{\chi}(\mathbf{q})\varepsilon^{*}\left(\frac{\tilde{c}A^{(2)}+\tilde{d}A^{(3)}}{q^2}+\frac{\tilde{c}C^{(2)}+\tilde{d}C^{(3)}}{q^2+(1/l_1^2)}+\frac{\tilde{c}D^{(2)}+\tilde{d}D^{(3)}}{q^2+(1/l_2^2)}\right), \tag{21}$$

The complete shape information for the inclusion is contained within $\hat{\chi}(\mathbf{q})$ making other terms in Eq. (21) independent of the shape (and geometry) effects. Eq. (21) can now be used to evaluate the polarization field for inclusion of any geometry in Fourier space, if $\hat{\chi}(\mathbf{q})$ for that geometry is known.

For the spherical shape (as shown in Fig. 4a), the shape function has a simple form (Andreev and Downes, 1999)

$$\hat{\chi}(\mathbf{q},R)=\frac{4\pi}{q}\left(\frac{\sin(\mathbf{q}R)}{q^2}-\frac{R\cos(\mathbf{q}R)}{q^2}\right). \tag{22}$$

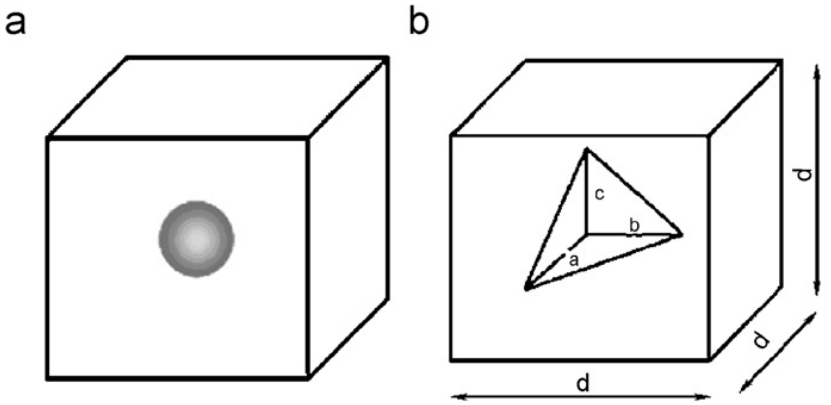

Fig. 4. Embedded inclusions (a) centrosymmetric (spherical) inclusion (b) non-centrosymmetric (orthogonal polyhedral) inclusion.

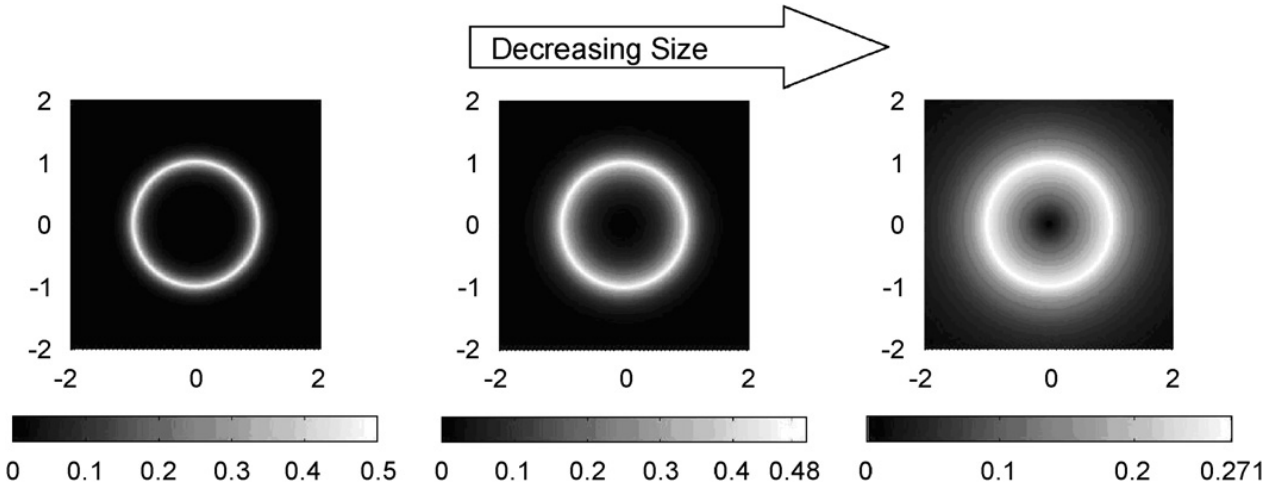

Fig. 5. Normalized contour plots of the electric fields around a spherical inclusion for different sizes subject to dilatational eigenstrain.

Here R is the radius of inclusion. Eq. (21) along with Eq. (22) may then be solved numerically using spectral method (Trefethen, 2000). A periodic distribution ($n_x d$, $n_y d$, $n_z d$) of inclusions is used. If a single inclusion solution is desired, a large cell-spacing must be employed to avoid interaction effects while (for eventual composite applications), the spacing may be adjusted to take into account finite volume fraction. Dimension d is normalized with the characteristic length-scale and each unit cell is uniformly meshed. A distribution of polarization field is thus obtained in the Fourier space which is then inverted back to the real space numerically. Thus contour-plots of the normalized electric fields distribution as a function of size and material property combinations (i.e. different combination of the characteristic lengths) for a spherical inclusion under dilatational strain may be obtained. Of course, for spherical geometry, analytical expressions for the potentials are available which can be directly used to generate such contour-plots which are shown here in Fig. 5. The numerical scheme described above is however general and essential for shapes other than spherical or cylindrical.

In Fig. 5, darker regions indicate low concentration of polarization while a lighter shade indicates a higher concentration of polarization. The material is non-piezoelectric and yet due to the presence of strain gradients, there exists a finite polarization in and around the

inclusion. As the size increases, the electric field becomes increasingly localized in thinner and thinner layers at the interface. Unlike the points at the interface, the interior points of the inclusion exhibit appreciable values only at sizes that are close to the flexoelectric characteristic length scales. To be more concrete and for illustration, we choose InAs–GaAs as an example inclusion-matrix system. Both are important quantum dot materials and subject to a large lattice mismatch induced dilatational transformation mismatch strain of ~6.7%. We then find that for an inclusion size of 5 nm, even far from the interface (i.e. a distance of 0.1 × radius from center), electric fields of hundreds of kV/m can be expected (this is in addition to the weakly classical piezoelectric effect in GaAs).

We should mention that spherical and such highly symmetric shapes are *useless* for obtaining effective piezoelectric coefficients from non-piezoelectric constituents. The high symmetry of such shapes ensures that the net averaged polarization vanishes globally although locally it is non-zero. These results are included here to bring about some of the qualitative nuances of the flexoelectric phenomenon.

As will be proved in Section 4, of real interest to the theme of the manuscript are inclusions of non-centrosymmetric shape. In Fig. 6 we plot contours of the numerically generated magnitude of the polarization field for orthogonal polyhedral shaped inclusion (shown in Fig. 4b) subject to a dilatational transformation strain. Characteristic shape function $\hat{\chi}(\mathbf{q})$ for the orthogonal polyhedral with a, b, c as the x, y, z-coordinate intercepts, respectively is easily derived to be

$$\hat{\chi}(\mathbf{q},a,b,c)=\frac{\left(\begin{array}{l}\mathrm{i}abe^{-\mathrm{i}cq_3}q_1q_2(aq_1-bq_2)+\mathrm{i}ace^{-\mathrm{i}bq_2}q_1q_3(cq_3-aq_1)\\ +\mathrm{i}bce^{-\mathrm{i}aq_1}q_2q_3(bq_2-cq_3)+(aq_1-bq_2)(bq_2-cq_3)(cq_3-aq_1)\end{array}\right)}{(aq_1-bq_2)(bq_2-cq_3)(cq_3-aq_1)}, \tag{23}$$

where q_1, q_2, q_3 are the wave vectors.

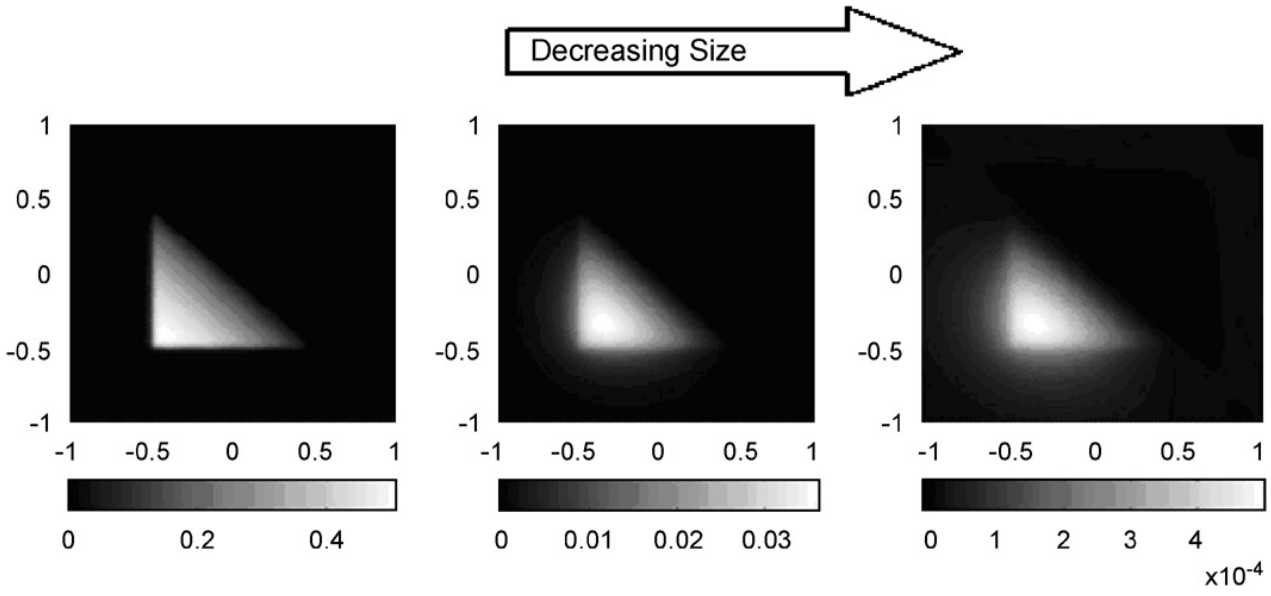

Fig. 6. Normalized contour plots of z-component of polarization around x–y plane of an orthogonal polyhedral inclusion for different sizes.

The size effect is evident as in the spherical case. With reduction in size, the electric field is seen to get denser in and around the inclusion. The distribution of the electric field is not symmetric. The *lack of centrosymmetry* in the distribution of polarization field results in a non-zero net averaged polarization in the inclusion (and thus by extension in the whole body). A notable observation is that if the inclusions were to be arranged in a *centrosymmetric topology* (say for example, randomly oriented), the averaged polarization will average to zero over the entire domain. Hence a proper arrangement of such *non-centrosymmetric shapes* and a *non-centrosymmetric topology* is necessary to generate non-zero average polarization. In the next section we formally provide this insight based on the mathematical structure of the governing equations.

4. Proposition: the requirement of material non-centrosymmetry for piezoelectricity in crystals is transferred to inhomogeneity shape and arrangement in flexoelectric continuum

Consider the case of a *centrosymmetric inhomogeniety* embedded inside an infinitely large medium.

Case 1: Applied voltage boundary condition as specified below exists

$$\phi(\mathbf{x})\big|_{\mathbf{x}=\text{¥}} = V, \quad \phi(\mathbf{x})\big|_{\mathbf{x}=-\text{¥}} = -V. \tag{24}$$

Since we have a centrosymmetric inhomogeneity, the boundary condition is anti-centrosymmetric in the potential '$\phi(\mathbf{x})$'. Thus, the solution of the potential '$\phi(\mathbf{x})$' will exhibit the same anti-centrosymmetry as that exhibited by the boundary condition. Then it follows that the potential '$\phi(\mathbf{x})$' is an odd function in $\mathbf{x}$:

$$\phi(\mathbf{x}) = -\phi(-\mathbf{x}). \tag{25}$$

Substituting the above condition in Eq. (9c), we observe that the polarization field must be an even function in '$\mathbf{x}$',[4] i.e.

$$\mathbf{P}(\mathbf{x}) = \mathbf{P}(-\mathbf{x}). \tag{26}$$

Further, substituting Eq. (25) into Eq. (9a), we observe that the displacement field '$\mathbf{u}(\mathbf{x})$' is also an even function in $\mathbf{x}$, i.e.

$$\mathbf{u}(\mathbf{x}) = \mathbf{u}(-\mathbf{x}). \tag{27}$$

As a result of the above symmetry requirement on the displacement field, the strain field '$\boldsymbol{\varepsilon}(\mathbf{x})$' is rendered an odd-function, i.e.

$$\boldsymbol{\varepsilon}(\mathbf{x}) = -\boldsymbol{\varepsilon}(-\mathbf{x}). \tag{28}$$

Thus the strain averaged over the volume of the system in the case of applied voltage condition is zero.

Case 2: Traction boundary condition exists as specified below

$$\boldsymbol{\sigma} \cdot \mathbf{n}|_{\mathbf{r}=S} = \mathbf{t}. \tag{29}$$

Once again, since the inhomogeneity is centrosymmetric, the given boundary condition is also centrosymmetric with respect to the stress '$\boldsymbol{\sigma}(\mathbf{x})$'. Thus, the solution of the stress function '$\boldsymbol{\sigma}(\mathbf{x})$' is also centrosymmetric. Then it follows that the stress '$\boldsymbol{\sigma}(\mathbf{x})$' is an even

[4]Here we have used the fact that the derivative of an odd function is an even function and vice versa.

function in $\mathbf{x}$. The stress field can be written in terms of the displacement and polarization fields as

$$\sigma_{ij}(\mathbf{x}) = c_{12}\delta_{ij}u_{k,k}(\mathbf{x}) + c_{44}\big(u_{i,j}(\mathbf{x}) + u_{j,i}(\mathbf{x})\big) + d_{12}\delta_{ij}P_{k,k}(\mathbf{x}) + d_{44}\big(P_{i,j}(\mathbf{x}) + P_{j,i}(\mathbf{x})\big). \tag{30}$$

Since $\boldsymbol{\sigma}(\mathbf{x})$ is even in $\mathbf{r}$ we can infer that

$$\begin{aligned} &c_{12}\delta_{ij}u_{k,k}(\mathbf{x}) + c_{44}\big(u_{i,j}(\mathbf{x}) + u_{j,i}(\mathbf{x})\big) + d_{12}\delta_{ij}P_{k,k}(\mathbf{x}) + d_{44}\big(P_{i,j}(\mathbf{x}) + P_{j,i}(\mathbf{x})\big) \\ &\quad = c_{12}\delta_{ij}u_{k,k}(-\mathbf{x}) + c_{44}\big(u_{i,j}(-\mathbf{x}) + u_{j,i}(-\mathbf{x})\big) + d_{12}\delta_{ij}P_{k,k}(-\mathbf{x}) \\ &\qquad + d_{44}\big(P_{i,j}(-\mathbf{x}) + P_{j,i}(-\mathbf{x})\big). \end{aligned} \tag{31}$$

From Eq. (9a) we observe that $\mathbf{u}(\mathbf{x})$ and $\mathbf{P}(\mathbf{x})$ have to be either both odd or both even. One can easily verify that if one of them is odd and the other function is even (or vice versa) then Eq. (9a) can never be satisfied. Further, from Eq. (27) we deduce that $\mathbf{u}(\mathbf{x})$ and $\mathbf{P}(\mathbf{x})$ have to be both odd. Since $\mathbf{P}(\mathbf{x})$ is odd, the polarization averaged over the volume of the system becomes zero.

Thus, to obtain effective piezoelectric behavior *without using piezoelectric constituents,* the symmetry of the internal arrangement must be chosen carefully. Any topology that has symmetry of transverse isotropy or less will yield a net overall polarization due to this effect (higher symmetry cannot sustain odd-order tensors that characterize the topology). In other words, *the requirement of material non-centrosymmetry for naturally occurring piezoelectrics is transferred to a requirement of shape/topology non-centrosymmetry in flexoelectric media*. Hence, for example, 2-layer laminate or the conical particle reinforced thin film shown in Fig. 3 are candidates that can demonstrate this effect.

5. Homogenization scheme for apparently piezoelectric composites

In this section we present a simple homogenization scheme that allows us to quantitatively, albeit approximately, estimate the effective piezoelectric behavior of a nanocomposite that is not comprised of piezoelectric materials. Our goal in the present manuscript is to demonstrate this central idea rather than develop a rigorous homogenization theory hence the simplest possible approach is employed.

Consider an infinite non-piezoelectric matrix containing an arbitrary shaped inhomogeneity subject to a far-field uniform strain, $\boldsymbol{\varepsilon}^{\infty}$. The Navier-like equations (Eqs. (9a–c)) may be re-written in an alternative form as

$$\begin{aligned} &\nabla(\mathbf{C} : \boldsymbol{\varepsilon} + \mathbf{D} : \nabla\mathbf{P}) + \mathbf{F} = 0, \\ &\nabla(\mathbf{D} : \boldsymbol{\varepsilon} + \mathbf{B} : \nabla\mathbf{P}) - \nabla\phi + \mathbf{E}^0 = 0, \\ &-\varepsilon_0\nabla^2\phi + \nabla\mathbf{P} = 0. \end{aligned} \tag{32a–c}$$

We define the position-dependent material properties as

$$\begin{aligned} &\mathbf{C}(\mathbf{x}) = \mathbf{C}^m + (\mathbf{C}^i - \mathbf{C}^m) : \mathbf{H}(\mathbf{x}) \Rightarrow \mathbf{C}^m + [\mathbf{C}] : \mathbf{H}(\mathbf{x}), \\ &\mathbf{D}(\mathbf{x}) = \mathbf{D}^m + [\mathbf{D}] : \mathbf{H}(\mathbf{x}), \\ &\mathbf{B}(\mathbf{x}) = \mathbf{B}^m + [\mathbf{B}] : \mathbf{H}(\mathbf{x}), \end{aligned} \tag{33}$$

where

$$\mathbf{H}(\mathbf{x}) = \begin{cases} \mathbf{1} \ldots \mathbf{x} \in V, \\ \mathbf{0} \ldots \mathbf{x} \notin V, \end{cases}$$

$\mathbf{C}^m$, $\mathbf{D}^m$, $\mathbf{B}^m \rightarrow$ Material property tensors for matrix,

$\mathbf{C}^i$, $\mathbf{D}^i$, $\mathbf{B}^i \rightarrow$ Material Property tensors for the inhomogeneity, and

$[\ ] =$ difference between properties of the matrix and the inhomogeneity. (34)

Hence Eq. (27a) becomes

$$\begin{aligned} &\nabla\{\mathbf{C}(\mathbf{x}) : \boldsymbol{\varepsilon} + \mathbf{D}(\mathbf{x}) : \nabla\mathbf{P}\} = \mathbf{0} \\ &\Rightarrow \nabla\{\mathbf{C}^m : \boldsymbol{\varepsilon} + [\mathbf{C}] : \boldsymbol{\varepsilon}\,\mathbf{H}(\mathbf{x}) + \mathbf{D}^m : \nabla\mathbf{P} + [\mathbf{D}] : \mathbf{P}\mathbf{H}(\mathbf{x})\} \\ &\Rightarrow \nabla\{\mathbf{C}^m : \boldsymbol{\varepsilon}\} + \nabla\{[\mathbf{C}] : \boldsymbol{\varepsilon}\,\mathbf{H}(\mathbf{x})\} + \nabla\{\mathbf{D}^m : \nabla\mathbf{P}\} + \nabla\{[\mathbf{D}] : \nabla\mathbf{P}\mathbf{H}(\mathbf{x})\} \\ &\Rightarrow \nabla\{\mathbf{C}^m : \boldsymbol{\varepsilon} + \mathbf{D}^m : \nabla\mathbf{P}\} + \underbrace{[\mathbf{C}] : \boldsymbol{\varepsilon}\,\delta(S) + [\mathbf{D}] : \nabla\mathbf{P}\delta(\mathbf{S})}_{=\text{Body Force}} = \mathbf{0}. \end{aligned} \tag{35}$$

Similarly

$$\begin{aligned} &\nabla\{\mathbf{D}(\mathbf{x}) : \boldsymbol{\varepsilon} + \mathbf{B}(\mathbf{x}) : \nabla\mathbf{P}\} = \mathbf{0} \\ &\Rightarrow \nabla\{\mathbf{D}^{\mathbf{m}} : \boldsymbol{\varepsilon} + \mathbf{B}^{\mathbf{m}} : \nabla\mathbf{P}\} + \underbrace{[\mathbf{D}] : \boldsymbol{\varepsilon}\delta(S) + [\mathbf{B}] : \nabla\mathbf{P}\delta(S)}_{=\text{Body Electric Field}} = \mathbf{0}. \end{aligned} \tag{36}$$

Thus an inhomogeneity within a matrix can be modeled as a fictitious body force and a fictitious body electric field. As customary in micromechanics (and already demonstrated in Section 3), the displacement $\mathbf{u}$ and polarization $\mathbf{P}$ can be expressed in terms of the derived Green's functions as

$$\mathbf{u} = \mathbf{u}^{\infty} - \int_{V'} \mathbf{G}^1 \nabla \cdot \{[\mathbf{C}] : \boldsymbol{\varepsilon}(\mathbf{x}')\}\,\mathrm{d}V' - \int_{V'} \mathbf{G}^2 \nabla \cdot \{[\mathbf{D}] : \nabla\mathbf{P}(\mathbf{x}')\}\,\mathrm{d}V' \tag{37}$$

and

$$\mathbf{P}(\mathbf{x}) = \mathbf{P}^{\infty} - \int_{V'} \mathbf{G}^3 \nabla \cdot \{[\mathbf{D}] : \boldsymbol{\varepsilon}(\mathbf{x}')\}\,\mathrm{d}V' - \int_{V'} \mathbf{G}^4 \nabla \cdot \{[\mathbf{B}] : \nabla\mathbf{P}(\mathbf{x}')\}\,\mathrm{d}V'. \tag{38}$$

Employing Gauss theorem and discarding the boundary terms, we obtain

$$\begin{aligned} u_i(\mathbf{x}) = u_i^{\infty} &+ \int_{V'} \left\{ G^1_{ji}(\mathbf{y}' - \mathbf{x}') \right\}_{,l} \{[C_{klmn}]\varepsilon_{mn}(\mathbf{x}')\}\,\mathrm{d}V' \\ &+ \int_{V'} \left\{ G^2_{ji}(\mathbf{y}' - \mathbf{x}') \right\}_{,l} \{[D_{klmn}]P_{m,n}(\mathbf{x}')\}\,\mathrm{d}V', \end{aligned} \tag{39}$$

$$\begin{aligned} P_i(\mathbf{x}) = P_i^{\infty} &+ \int_{V'} \left\{ G^3_{ji}(\mathbf{y}' - \mathbf{x}') \right\}_{,l} \{[D_{jlmn}]\varepsilon_{mn}(\mathbf{x}')\}\,\mathrm{d}V' \\ &+ \int_{V'} \left\{ G^4_{ji}(\mathbf{y}' - \mathbf{x}') \right\}_{,l} \{[B_{jlmn}]P_{m,n}(\mathbf{x}')\}\,\mathrm{d}V'. \end{aligned} \tag{40}$$

The strain field is then

$$\varepsilon_{ij}(\mathbf{x}) = \varepsilon_{ij}^{\infty} + \tfrac{1}{2}\int_{V'}\left\{G^1_{jk,li}(\mathbf{y}'-\mathbf{x}') + G^1_{ik,lj}(\mathbf{y}'-\mathbf{x}')\right\}\{[C_{klmn}]\varepsilon_{mn}(\mathbf{x}')\}\,\mathrm{d}V' + \tfrac{1}{2}\int_{V'}\left\{G^2_{jk,li}(\mathbf{y}'-\mathbf{x}') + G^2_{ik,lj}(\mathbf{y}'-\mathbf{x}')\right\}\{[D_{klmn}]P_{m,n}(\mathbf{x}')\}\,\mathrm{d}V'. \tag{41}$$

Eqs. (40) and (41) are integral equations that must be solved to determine the polarization and strain states of an unbounded body containing an inhomogeneity under the extended theory of electromechanical coupling that incorporate flexoelectricity. In classical elasticity (for ellipsoidal shape), the strain is uniform within the inhomogeneity and thus allows one to take the strain field out of the integral sign effectively converting the integral equation into an algebraic one. This is not possible in our case as both strain and polarization are inhomogeneous (even for ellipsoidal shape) let alone for non-centrosymmetric shapes that are relevant in the present context. Thus, a suitable approximation must be found to solve Eqs. (40) and (41) and evaluate the average polarization.

A perturbation type approach (cf. Markov, 1979 in the context of micropolar solids) can be used to solve these integral equations. As a first approximation we may assume that the actual strain (polarization field) to be the average uniform strain (polarization field). This approximation is merely the first term in the perturbation series involving the difference between the matrix-inhomogeneity moduli—the next order approximation, as it turns out, was found to be negligible (see Appendix B). Subject to this assumption, Eqs. (41) and (40), respectively, become

$$\varepsilon_{ij}(\mathbf{x}) \approx \varepsilon_{ij}^{\infty} + \tfrac{1}{2}\int_{V'}\left\{G^1_{jk,li}(\mathbf{y}'-\mathbf{x}') + G^1_{ik,lj}(\mathbf{y}'-\mathbf{x}')\right\}\{[C_{klmn}]\langle\varepsilon_{mn}\rangle\}\,\mathrm{d}V' + \tfrac{1}{2}\int_{V'}\left\{G^2_{jk,li}(\mathbf{y}'-\mathbf{x}') + G^2_{ik,lj}(\mathbf{y}'-\mathbf{x}')\right\}\{[D_{klmn}]\langle P_{m,n}\rangle\}\,\mathrm{d}V',$$

$$P_i(\mathbf{x}) = P_i^{\infty} + \int_{V'} G^3_{ki,l}(\mathbf{y}'-\mathbf{x}')[D_{klmn}]\langle\varepsilon_{mn}\rangle\,\mathrm{d}V' + \int_{V'} G^4_{ki,l}(\mathbf{y}'-\mathbf{x}')[B_{klmn}]\langle P_{m,n}\rangle\,\mathrm{d}V'. \tag{42a–b}$$

Further, taking average values over V on both sides in these equations, we obtain

$$\langle\varepsilon_{ij}\rangle \approx \varepsilon_{ij}^{\infty} + \tfrac{1}{2}\left\langle\int_{V'}\left\{G^1_{jk,li}(\mathbf{y}'-\mathbf{x}') + G^1_{ik,lj}(\mathbf{y}'-\mathbf{x}')\right\}\mathrm{d}V'\right\rangle[C_{klmn}]\langle\varepsilon_{mn}\rangle + \tfrac{1}{2}\left\langle\int_{V'}\left\{G^2_{jk,li}(\mathbf{y}'-\mathbf{x}') + G^2_{ik,lj}(\mathbf{y}'-\mathbf{x}')\right\}\mathrm{d}V'\right\rangle[D_{klmn}]\langle P_{m,n}\rangle,$$

$$\langle P_i\rangle = P_i^{\infty} + \left\langle\int_{V'} G^3_{ki,l}(\mathbf{y}'-\mathbf{x}')\,\mathrm{d}V'\right\rangle[D_{klmn}]\langle\varepsilon_{mn}\rangle + \left\langle\int_{V'} G^4_{ki,l}(\mathbf{y}'-\mathbf{x}')\,\mathrm{d}V'\right\rangle[B_{klmn}]\langle P_{m,n}\rangle. \tag{43a–b}$$

Further algebraic manipulations lead to following expressions in terms of the material constants, potentials (Eqs. (17a–c)) and the average strains:

$$\left\langle\varepsilon_{ij}\right\rangle \approx \varepsilon_{ij}^{\infty} + \left\langle\left\{\Omega^{(1)}_{iklj} + \frac{\delta_{ik}\Omega^{(2)}_{lj} + \delta_{jk}\Omega^{(2)}_{li}}{2} - \Omega^{(3)}_{iklj}\right\}\right\rangle[C_{klmn}]\langle\varepsilon_{mn}\rangle, \tag{44}$$

where

$$\Omega^{(1)}_{iklj} = A^{(1)}\phi_{,iklj} - \frac{B^{(1)}}{2}\psi_{,iklj} + C^{(1)}M^{1}_{,iklj} + D^{(1)}M^{2}_{,iklj},$$
$$\Omega^{(2)}_{lj} = E^{(1)}\phi_{,lj} + F^{(1)}M^{3}_{,lj} + G^{(1)}M^{4}_{,lj},$$
$$\Omega^{(3)}_{iklj} = \frac{E^{(1)}}{2}\psi_{,iklj} - \left(F^{(1)}l_3^2 + G^{(1)}l_4^2\right)\phi_{,iklj} + \left(F^{(1)}l_3^2M^{3}_{,iklj} + G^{(1)}l_4^2M^{4}_{,iklj}\right)$$

and

$$\langle P_i\rangle \approx P_i^{\infty} + \left\langle \Omega^{(4)}_{kil} + \delta_{ki}\Omega^{(5)}_{l} - \Omega^{(6)}_{kil}\right\rangle [D_{klmn}]\langle\varepsilon_{mn}\rangle, \tag{45}$$

where

$$\Omega^{(4)}_{kil} = A^{(2)}\phi_{,kil} + C^{(2)}M^{1}_{,kil} + D^{(2)}M^{2}_{,kil},$$
$$\Omega^{(5)}_{l} = F^{(2)}M^{3}_{,l} + G^{(2)}M^{4}_{,l},$$
$$\Omega^{(6)}_{kil} = \left(F^{(2)}l_3^2M^{3}_{,kil} + G^{(2)}l_4^2M^{4}_{,kil}\right) - \left(F^{(2)}l_3^2 + G^{(2)}l_4^2\right)\phi_{,kil}.$$

Eq. (44) represents a system of six simultaneous algebraic equations in components of $\langle\boldsymbol{\varepsilon}\rangle$ while Eq. (45) provides the three components of polarization field $\langle\mathbf{P}\rangle$.

Now, Eqs. (43a–b) involve integration over volume V' of the transformed inclusion. Thus the shape of the inhomogeneity has strong bearing over the polarization and strain fields. As discussed in Section 3, separating the shape effect in the form of a characteristic shape function $\hat{\chi}(\mathbf{q})$ the strain and polarization fields (Eqs. (43a–b)) in Fourier space become

$$\widehat{\langle\varepsilon_{ij}\rangle} \approx \varepsilon_{ij}^{\infty} - \tfrac{1}{2}\left\langle\left(q_lq_i\widehat{G^{1}_{jk}} + q_lq_j\widehat{G^{1}_{ik}}\right)\right\rangle [C_{klmn}]\widehat{\langle\varepsilon_{mn}\rangle}\hat{\chi}(\mathbf{q}),$$
$$\widehat{\langle P_i\rangle} \approx P_i^{\infty} + \left\langle\left(\mathrm{i}q_l\widehat{G^{3}_{ki}}\right)\right\rangle [D_{klmn}]\widehat{\langle\varepsilon_{mn}\rangle}\hat{\chi}(\mathbf{q}). \tag{46a–b}$$

Substituting Eqs. (17a–c) in Eqs. (43a–b), we obtain the following analytical expressions for strain and polarization

$$\widehat{\langle\boldsymbol{\varepsilon}\rangle} \approx \left(\boldsymbol{I} - \left\langle\widehat{\boldsymbol{\Gamma}^{(1)}}(\mathbf{q})\right\rangle[\mathbf{C}]\hat{\chi}(\mathbf{q})\right)^{-1}\boldsymbol{\varepsilon}^{\infty}$$

and

$$\widehat{\langle\mathbf{P}\rangle} \approx \mathbf{P}^{\infty} + \left\langle\widehat{\boldsymbol{\Gamma}^{(2)}}(\mathbf{q})\right\rangle[\mathbf{D}]\widehat{\langle\boldsymbol{\varepsilon}\rangle}\hat{\chi}(\mathbf{q}). \tag{47a–b}$$

Here $\boldsymbol{I}$ is the fourth-order identity tensor and

$$\widehat{\Gamma^{(1)}_{iklj}}(\mathbf{q}) = q_lq_j\left(-\frac{C^{(11)}q_iq_k}{\mathbf{q}^2 + l_1^2\mathbf{q}^4} - \frac{2C^{(01)}\left(-1 + q_iq_k\right)}{\mathbf{q}^4} + \frac{C^{(12)} - C^{(22)}q_iq_k}{\mathbf{q}^2 + l_2^2\mathbf{q}^4}\right), \tag{48}$$

$$\widehat{\Gamma^{(2)}_{kil}}(\mathbf{q}) = \frac{\mathrm{i}q_l\left(q_kq_iC^{(21)}\left(1 + l_2^2\mathbf{q}^2\right) + \left(-1 + q_kq_i\right)C^{(22)}\left(1 + l_1^2\mathbf{q}^2\right)\right)}{\mathbf{q}^2\left(1 + l_1^2\mathbf{q}^2\right)\left(1 + l_2^2\mathbf{q}^2\right)}. \tag{49}$$

Eqs. (47b) along with Eq. (47a) must be solved numerically using spectral method (Trefethen, 2000) as described in Section 3. It is important to note that the unit cell used in the numerical spectral calculations is periodic. The relative sizes of the inhomogeneity and the unit

cell define the volume fraction of the composite (e.g. in Fig. 4b, ratio of volume of tetrahedron ($(\frac{1}{6})abc$) to volume of unit cell (d^3) defines the volume fraction). Changing the inhomogeneity size for the fixed size of unit-cell allows us to account for various volume fractions.

6. Numerical results

The homogenization scheme developed in the previous section is applied to the orthogonal polyhedral shape inhomogeneity in Fig. 4b. Currently the availability of flexoelectric properties for different materials is a major bottleneck. Askar et al. (1970) list the isotropic material properties derived from a lattice dynamical model for alkali halides, in particular NaCl and KCl. Obviously these materials are not the best choice for a composite system however our purpose in this work is merely illustrative hence we will employ properties that correspond to these materials with the caveat that in the future (once properties for other dielectric solids have been determined) more practical systems will be investigated. In principle all dielectric combinations will lead to similar qualitative results. Currently efforts are in progress to evaluate flexoelectric material properties via quantum mechanical Berry phase calculations for various technologically relevant dielectrics.

Numerically calculated values for the z-component of the polarization (normalized with respect to quartz) for different volume fractions are shown in Fig. 7 as a function of the inhomogeneity size. Inhomogeneity size is indicated by the dimension of one of the sides of tetrahedron. As expected, the average polarization vanishes as the size of the inhomogeneity is increased (corresponding to smaller and smaller strain gradients).

Qualitatively, the following can be inferred: assume that the volume fraction of the second phase is negligibly small. Then, the average strain gradients will also be small and

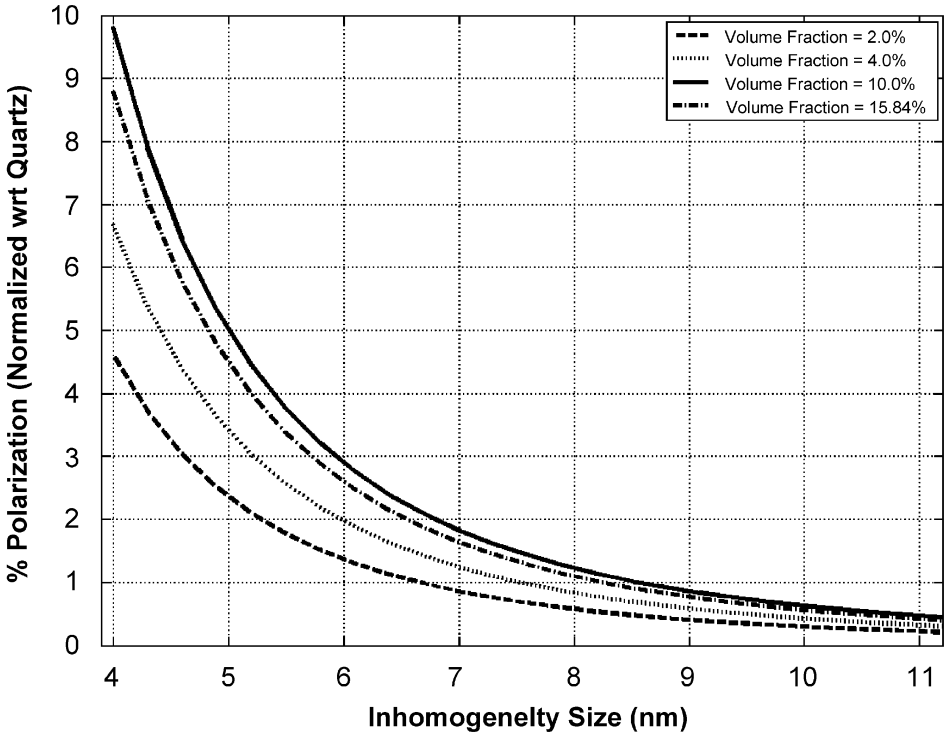

Fig. 7. The z-component of the polarization (normalized with respect to quartz) as a function of inclusion size for a tetrahedral inhomogeneity depicted in Fig. (4b). Note that amongst the four different volume fractions considered (2.0%, 4.0%, 10.0% and 15.84%), maximum polarization is observed for a volume fraction of 10%.

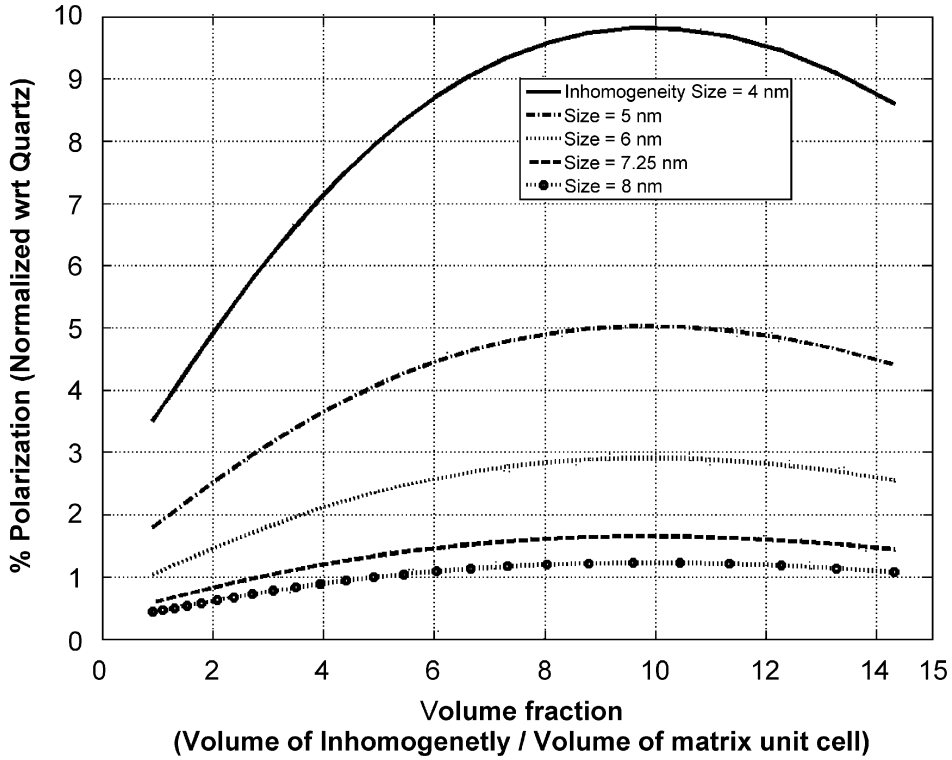

Fig. 8. The z-component of the polarization (normalized with respect to quartz) as a function of volume fraction of the composite with tetrahedral inhomogeneity of non-piezoelectric material in non-piezoelectric matrix.

one will obtain negligible overall piezoelectric behavior. Now consider the other extreme: the volume fraction is very high. Once again, due to large fraction of one phase, strain state will become increasingly homogeneous and overall electromechanical coupling will once again be small. Thus it can be expected that the induced polarization be extremely small for low concentrations of either of the constituents while it will increase and reach a maximum at some intermediate volume fraction. This simple qualitative argument alludes to the fact that for a given topology arrangement and material combination there exists an "*optimum*" volume fraction for which a maximal overall electromechanical coupling will be observed. The effect of the volume fraction on the z-component of polarization is explicitly shown in Fig. 8. We note that for the given inhomogeneity, the maximum allowed volume fraction is 16.67%, at which the inhomogeneity edge is of the same length as that of the matrix unit cell. This opens up the prospects for search of optimum size of the inclusion and the optimum volume fraction of the composite.

Given the properties we have chosen—see Appendix A, due to low elastic and dielectric contrast and relatively low flexoelectric coefficients a maximum of 10% of Quartz polarization is achieved. Considering that solely non-piezoelectric materials are used, these numbers are tantalizing and may be easily improved upon (and calculated using the developed model in our paper) for other materials.

7. Conclusion and summary

In summary, the universal strain gradient—polarization coupling also known as flexoelectricity—may be employed to create apparently piezoelectric nanocomposites without using piezoelectric materials. Even for a rather poor choice of materials (due to

limited data availability) we find that close to 10% of Quartz electromechanical performance can be obtained in the size regime of 4–5 nm. We expect that future work will focus on evaluation of the flexoelectric coefficients of various technologically relevant dielectrics and consequently optimum design of a new class of piezoelectric meta-materials. Currently the authors are attempting to use Berry-phase quantum mechanical approach to evaluate the flexoelectric coefficients and will be reported in future publications. On the theoretical side, there is a need for the further development of rigorous homogenization schemes for the new classes of coupled electromechanical equations discussed in the present work.

Acknowledgments

Discussions with Xinyuan Zhang are gratefully acknowledged. PS and RM acknowledge support from Office of Naval Research while support for NDS is provided by Texas ARP.

Appendix A

The coefficients $C^{(ij)}$ in the Green's functions defined in Eqs. (13a–c) are:

$$C^{(01)} = \frac{c_{44}+c_{12}}{2c_{44}(c_{12}+2c_{44})}, \quad C^{(02)} = \frac{1}{2c_{44}}, \quad C^{(11)} = \frac{d_{11}^2}{\left(a+\varepsilon_0^{-1}\right)c_{11}^2},$$
$$C^{(12)} = \frac{d_{44}^2}{ac_{44}^2}, \quad C^{(21)} = -\frac{d_{11}}{\left(a+\varepsilon_0^{-1}\right)c_{11}}, \quad C^{(21)} = \frac{d_{44}}{ac_{44}} \tag{A.1}$$

while

$$I_a = \frac{\left(\exp(-R/l_a)-1\right)}{R}. \tag{A.2}$$

In the above equation l_1 and l_2 are new length scale parameters which are defined in terms of the material coefficients as

$$l_1^2 = \frac{b_{11} - \frac{(d_{11}-f_{11})^2}{c_{11}}}{\left(a+\varepsilon_0^{-1}\right)}, \quad l_2^2 = \frac{(b_{44}+b_{77}) - \frac{(d_{44}-f_{12})^2}{c_{44}}}{a}. \tag{A.3}$$

Material Constants for NaCl and KCl are (Askar et al., 1971):

		NaCl	KCl
c_{12}	$10^{12}\,\mathrm{dyn/cm^2}$	0.148	0.105
c_{44}		0.149	0.105
D_{12}	$10^{7}\,\mathrm{dyn\text{-}cm/C}$	0.470	0.392
D_{44}		−0.170	−0.178
B_{12}	$10^{4}\,\mathrm{dyn\text{-}cm^4/C^2}$	-1.6×10^{-7}	-25.6×10^{-7}
B_{44}		0.344	0.600
B_{77}		0.344	0.600
A	$10^{19}\,\mathrm{dyn\text{-}cm^2/C^2}$	1.74	2.43
l_1^2	$10^{-16}\,\mathrm{cm^2}$	0.527	0.873
c_{44}		3.943	4.926

and

$$c_{11} = c_{12} + 2c_{44}, \quad d_{11} = d_{12} + 2d_{44}, \quad b_{11} = b_{12} + 2b_{44}.$$

Appendix B. Higher-order approximation for $\boldsymbol{\varepsilon}(\mathbf{x}')$

We assumed $\boldsymbol{\varepsilon}(\mathbf{x}')$ and $\mathbf{P}(\mathbf{x}')$ to be constant within the inhomogeneity so that $\boldsymbol{\varepsilon}(\mathbf{x}') = \langle \boldsymbol{\varepsilon} \rangle$ and $\mathbf{P}(\mathbf{x}') = \langle \mathbf{P} \rangle$. This is the first-order approximation. A series expansion of the strain field can be a better approximation. Let

$$\begin{aligned} \varepsilon_{ij}(\mathbf{x}') &= \langle \varepsilon_{ij} \rangle + {}^{\varepsilon}a_{ijk}x'_k + {}^{\varepsilon}b_{ijkl}x'_k x'_l + \cdots, \\ P_{i,j}(\mathbf{x}') &= \langle P_{i,j} \rangle + {}^{p}a_{ijk}x'_k + {}^{p}b_{ijkl}x'_k x'_l + \cdots, \end{aligned} \tag{B.1}$$

where ${}^{\varepsilon}a_{ijk}$, ${}^{p}a_{ijk}$, ${}^{\varepsilon}b_{ijkl}$, ${}^{p}b_{ijkl}$, ... are constants to be determined by solving following algebraic equations: Choosing up to second term, we can write Eqs. (41) and (40), respectively, as

$$\begin{aligned} \varepsilon_{ij}(\mathbf{x}) \approx \varepsilon_{ij}^{\infty} &+ \tfrac{1}{2}\int_{V'} \left\{ G^1_{jk,li}(\mathbf{y}' - \mathbf{x}') + G^1_{ik,lj}(\mathbf{y}' - \mathbf{x}') \right\} \left\{ [C_{klmn}] \left(\langle \varepsilon_{mn} \rangle + {}^{\varepsilon}a_{ijk}x'_k \right) \right\} \mathrm{d}V' \\ &+ \tfrac{1}{2}\int_{V'} \left\{ G^2_{jk,li}(\mathbf{y}' - \mathbf{x}') + G^2_{ik,lj}(\mathbf{y}' - \mathbf{x}') \right\} \left\{ [D_{klmn}] \left(\langle P_{m,n} \rangle + {}^{p}a_{ijk}x'_k \right) \right\} \mathrm{d}V', \\ P_i(\mathbf{x}) \approx P_i^{\infty} &+ \int_{V'} G^3_{ki,l}(\mathbf{y}' - \mathbf{x}')[D_{klmn}] \left(\langle \varepsilon_{mn} \rangle + {}^{\varepsilon}a_{ijk}x'_k \right) \mathrm{d}V' \\ &+ \int_{V'} G^4_{ki,l}(\mathbf{y}' - \mathbf{x}')[B_{klmn}] \left(\langle P_{m,n} \rangle + {}^{p}a_{ijk}x'_k \right) \mathrm{d}V'. \end{aligned} \tag{B.2}$$

The polarization field with this higher-order approximation can be calculated following the same approach as described in Section 5. Our numerical analysis for the second-order approximation shows that only a minor improvement is obtained for the given material properties. This conclusion may change if the elastic or dielectric contrast is large.

References

Andreev, A.D., Downes, J.R., 1999. Strain distributions in quantum dots of arbitrary shape. J. Appl. Phys. 86, 297–305.

Askar, A., Lee, P.C.Y., Cakmak, A.S., 1970. Lattice dynamics approach to the theory of elastic dielectrics with polarization gradients. Phys. Rev. B 1, 3525–3527.

Askar, A., Lee, P.C.Y., Cakmak, A.S., 1971. The effect of surface curvature and discontinuity on the surface energy density and other induced fields in elastic diaelectrics. Int. J. Solids Struct. 7, 523–537.

Askar, A., Lee, P.C.Y., 1970. Lattice dynamics approach to the theory of diatomic elastic dielectrics. Phys. Rev. B 9 (12), 5291–5299.

Bauer, C.L., Brantley, W.A., 1970. Effect of charged dislocations on a.c. dielectric and elastic properties. Mater. Sci. Eng. 5, 295–297.

Bursian, E.V., Trunov, N.N., 1974. Nonlocal piezoelectric effect. Fiz. Tverd. Tela 16, 1187–1190.

Catalan, G., Sinnamon, L.J., Gregg, J.M., 2004. The effect of flexoelectricity on the dielectric properties of inhomogeneously strained ferroelectric thin films. J. Phys. Condens. Matter 16, 2253–2264.

Cheng, Z.Q., He, L.H., 1997. Micropolar elastic fields due to a spherical inclusion. Int. J. Eng. Sci. 33, 389–397.

Cochran, W., Cowley, R.A., 1962. Dielectric constants and lattice vibrations. Phys. Chem. Solids 23, 447–450.

Cross, L.E., 2006. Flexoelectric effects: charge separation in insulating solids subjected to elastic strain gradients. J. Mater. Sci. 41, 53–63.

Dick, B.J., Overhauser, A.W., 1958. Theory of the dielectric constants of alkali halide crystals. Phys. Rev. 112, 90–103.

Dumitrica, T., Landis, C.M., Yakobson, B.I., 2002. Curvature induced polarization in carbon nanoshells. Chem. Phys. Lett. 360, 182–188.

Eshelby, J.D., 1957. The determination of the elastic field of an ellipsoidal inclusion, and related problems. Proc. R. Soc. London A 241, 376–396.

Fousek, J., Cross, L.E., Litvin, D.B., 1999. Possible piezoelectric composites based on flexoelectric effect. Mater. Lett. 39, 289–291.

Gibbons, G.W., Whiting, B.F., 1981. Newtonian gravity measurements impose constraints on unification theories. Nature 291, 636–638.

Indenbom, V.L., Loginov, V.B., Osipov, M.A., 1981. Flexoelectric effect and structure of crystals. Kristallografiya 28, 1157–1162.

Kleinert, H., 1989. Gauge Fields in Condensed Matter, Vol. II, Stresses and Defects. World Scientific, Singapore.

Kogan, Sh.M., 1963. Piezoelectric effect under an inhomogeneous strain and acoustic scattering of carriers in crystals. Fiz. Tverd. Tela 5 (10), 2829–2831.

Ma, W., Cross, L.E., 2001a. Observation of the flexoelectric effect in relaxor Pb(Mg1/3Nb2/3)O3 ceramics. Appl. Phys. Lett. 78 (19), 2920–2921.

Ma, W., Cross, L.E., 2001b. Large flexoelectric polarization in ceramic lead magnesium niobate. Appl. Phys. Lett. 79 (19), 4420–4422.

Ma, W., Cross, L.E., 2002. Flexoelectric polarization in barium strontium titanate in the paraelectric state. Appl. Phys. Lett. 81 (19), 3440–3442.

Ma, W., Cross, L.E., 2003. Strain-gradient induced electric polarization in lead zirconate titanate ceramics. Appl. Phys. Lett. 82 (19), 3923–3925.

Maranganti, R., Sharma, N.D., Sharma, P., 2006. Electromechanical coupling in nonpiezoelectric materials due to nanoscale nonlocal size effects: Green's function solutions and embedded inclusions. Phys. Rev. B 74, 014110-1–014110-14.

Markov, K., 1979. On the inhomogeneity problem in micropolar elasticity. Theor. Appl. Mech. 3, 52–59.

Marvan, M., Havranek, A., 1988. Flexoelectric effect in elastomers. Prog. Colloid Polym. Sci. 78, 33–36.

Marvan, M., Havranek, A., 1997. Static volume flexoelectric effect in a model of linear chains. Solid State Commun. 101 (7), 493–496.

Maugin, G.A., 1988. Continuum Mechanics of Electromagnetic Solids. North-Holland, Amsterdam.

Meyer, R.B., 1969. Piezoelectric effects in liquid crystals. Phys. Rev. Lett. 22, 918–921.

Mindlin, R.D., 1968. Polarization gradient in elastic dielectrics. Int. J. Solids. Struct. 4, 637–642.

Mura, T., 1987. Micromechanics of Defects in Solids. Martinus Nijhoff, Hague, The Netherlands.

Nakhmanson, S.M., Calzolari, A., Meunier, V., Bernholc, J., Nardelli, M.B., 2003. Spontaneous polarization and piezoelectricity in boron nitride nanotubes. Phys. Rev. B 67, 235406–235410.

Nowacki, J.P., Hsieh, R.K.T., 1986. Lattice defects in linear isotropic dielectrics. Int. J. Eng. Sci. 24 (10), 1655–1666.

Nowick, A.S., Heller, W.R., 1965. Dielectric and anelastic relaxation of crystals containing point defects. Adv. Phys. (Suppl. Philos. Mag.) 14 (54), 101–166.

Nye, J.F., 1985. Physical Properties of Crystals: Their Representation by Tensors and Matrices, reprint ed. Oxford University Press, Oxford.

Robinson, W.H., Glover, A.J., Wolfenden, A., 1978. Electrical–mechanical coupling of dislocations in KCl, NaCl, LiF, and CaF2. Phys. Stat. Sol. (a) 48, 155–163.

Sahin, E., Dost, S., 1988. A strain-gradient theory of elastic dielectrics with spatial dispersion. Int. J. Eng. Sci. 26 (13), 1231–1245.

Schmidt, D., Schadt, M., Helfrich, W., 1972. Liquid-crystalline curvature electricity: the bending mode of MBBA. Z. Naturforsch. A 27a (2), 277–280.

Sharma, P., Ganti, S., Bhate, N., 2003. The effect of surfaces on the size- dependent elastic state of (nano) inhomogeneities. Appl. Phys. Lett. 82 (4), 535–537.

Tagantsev, A.K., 1986. Piezoelectricity and flexoelectricity in crystalline dielectrics. Phys. Rev. B 34 (8), 5883–5889.

Tagantsev, A.K., 1991. Electric polarization in crystals and its response to thermal and elastic perturbations. Phase Transit. 35 (3–4), 119–203.

Tolpygo, K.B., 1962. Investigation of long-wavelength vibrations of diamond-type crystals with an allowance for long-range forces. Sov. Phys.—Solid States 4 (7), 1765–1777.

Trefethen, L.N., 2000. Spectral Methods in Matlab. SIAM, Philadelphia.
Whitworth, R.W., 1964. Production of electrostatic potential differences in sodium chloride crystals by plastic compression and bending. Philos. Mag. 4 (107), 801–816.
Zhang, X., Sharma, P., 2005a. Inclusions and inhomogeneities in strain gradient elasticity with couple stresses and related problems. Int. J. Solids Struct. 42, 3833–3851.
Zhang, X., Sharma, P., 2005b. Size dependency of strain in arbitrary shaped, anisotropic embedded quantum dots due to nonlocal dispersive effects. Phys. Rev. B 72, 195345-1–195345-16.
Zheludev, I.S., Likhacheva, Y.U.S., Lileeva, N.A., 1969. Further contribution to the question of the electrical polarization of crystals by torsional deformation. Kristallografiya 14 (3), 514–516.
Zhu, W., Fu, J.Y., Li, N., Cross, L.E., 2006. Piezoelectric composite based on the enhanced flexoelectric effects. Appl. Phys. Lett. 89, 192904.